Journal of Materials Chemistry B

Accepted Manuscript

ROYAL SOCIETY OF CHEMISTRY

www.rsc.org/materialsB

Journal Name

RSCPublishing

ARTICLE

Development of a spatiotemporal method to control molecular function by using silica-based photodegradable nanoparticles

Cite this: DOI: 10.1039/x0xx00000x

Received 00th January 2012,
Accepted 00th January 2012

DOI: 10.1039/x0xx00000x

www.rsc.org/

Fumi Ishizuka,[1] Xiangsheng Liu,[2] Shuhei Murayama,[1, #] Tomofumi Santa,[1] and Masaru Kato,[1 *]

To effectively and safely use molecules, it is important to be able to control the timing and site of molecule activation. We developed a spatiotemporal method to control molecular function by using silica-based photodegradable nanoparticles that can be prepared under mild conditions. The function of various molecules, such as rhodamine B, Nile blue A, propidium iodide (PI), and rhodamine 110, bis-(*N*-CBZ-L-arginine amide), dihydrochloride (BZAR), was restricted by wrapping in the network structure of the nanoparticle gel. The encapsulated molecule was released from the gel by light stimulus and its function was restored. Hence, this technique is applicable to the functional control of various molecules. The PI-encapsulated nanoparticles were internalized by the cells after conjugated with the cell membrane permeability peptide, octaarginine, and were localized to the cytoplasm. Short-term irradiation (20 s) induced PI release from the nanoparticles and the rapid movement (less than 2 min) of the released PI to the nucleus. These nanoparticles are thus useful tools for the spatiotemporal control of various molecular functions because they permit the quick and transient release of encapsulated molecules after short-term irradiation and can be prepared under mild conditions.

Introduction

Each molecule has its own function(s) and modern society makes use of millions or perhaps billions of functional molecules. It is therefore essential to control the function of these molecules spatiotemporally for their use in daily life, because activation at the wrong place or time can sometimes lead to harmful effects.[1, 2] To control molecular function, external stimuli (e.g. light, heat, or a magnetic field) and stimulus-sensitive elements or groups have been used.[3, 4] Light has long been considered a suitable stimulus because of its excellent usability and selectivity, and many elements and molecules that are activated by light have been developed and used around the world. [5]

We previously developed a universal method to functionally control molecules by using a polyethylene glycol (PEG)-based photodegradable gel.[6,7] The molecular function can be restricted when the molecule is encapsulated within the gel and the activity is restored by releasing the molecule from the gel when collapse of the gel is induced by irradiation. Because the molecule is physically wrapped by the network structure of the gel, no chemical bonding is required for encapsulation using this technique. In addition, the mesh size of the gel can be modified by changing the size of the monomer, and the size range of the encapsulated molecule is broad (from small molecules like fluorescein (m.w. 389 Da) to large molecules like ferritin (m.w. 450k Da)). [8,9] We thought that this technique was applicable for the functional control of a variety of molecules and named it the "PARCEL" method (Scheme 1). Furthermore we found that the gel comprised 100-nm spherical nanoparticles when it was prepared by using a vortex for mixing.[10-12] Because photodegradable nanoparticles can serve as a vehicle to transport a molecule to a target place and release the cargo molecule at that place in response to a photo stimulus, the molecule-encapsulated nanoparticles were considered useful tools for the spatiotemporal control of molecular function. The quick and transient release of encapsulated molecules was also accomplished by irradiation, because collapse of the gel could be induced with a short burst of irradiation (as little as 10 seconds). Hence, the nanoparticles allow us to induce drastic changes in the concentration or amount of active molecule at the time of irradiation. We used nanoparticles to locally activate molecules within a cell and tried to clarify the effect of releasing that molecule within the cell; we also tried to control cellular functions using the released molecule. [10-12]

However, our recent studies indicate that some small molecules, such as Nile blue A and propidium iodide (PI), are not controlled correctly by the PARCEL method. We propose two hypotheses to explain the lack of control of some small molecules with the PARCEL method: 1) the mesh size of the gel prepared from PEG was too large to encapsulate the small molecule, or 2) the radical polymerization that was used to prepare the gel damaged the small molecule during preparation. To test these hypotheses, we examined silica gel prepared from the polymerization reaction of alkoxysilane. Because silica has

excellent biocompatibility, like PEG, and the mesh size of silica gel was small, silica-based photodegradable gel could be broadly applicable in this context. Moreover, our previous research suggested that silica gel offers the advantages of improved stability of the encapsulated molecule within the silica gel and that it can be prepared under mild conditions. [13-16] Therefore, in the present study we developed silica-based photodegradable nanoparticles and applied them to the spatiotemporal control of molecular function within the cell.

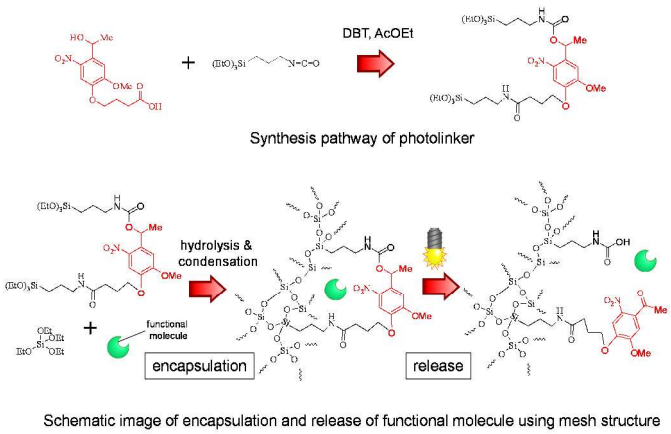

Scheme 1 Synthesis pathway of photolinker and an image of functional molecule encapsulation and release.

Experimental section

Materials

Arginine, Nile blue A, rhodamine B, 3-(triethoxysilyl)propyl isocyanate (IPS), dibutyltin (IV) dilaurate (DBT), hexane, potassium carbonate, DNA from salmon sperm and ethyl acetate were purchased from Wako Pure Chemical Industries (Osaka, Japan). 4-[4-(1-Hydroxyethyl)-2-methoxy-5-nitrophenoxy]butyric acid and octaarginine (R8) peptide were obtained from Sigma-Aldrich (St. Louis, MO). Tetraethyl orthosilicate (TEOS) was from Kojundo Chemical Laboratory (Saitama, Japan). Cyclohexane was from Tokyo Chemical Industry (Tokyo, Japan). Silica gel (0.063-0.210mm) was from Kanto Chemical co., inc, (Tokyo, Japan). SYTO16 and rhodamine 110, bis-(*N*-CBZ-L-arginine amide), dihydrochloride (BZAR) were from Invitrogen (Carlsbad, CA). Propidium iodide (PI) was form Dojindo (Kumamoto, Japan). Water was purified with a Milli-Q apparatus (Millipore, Bedford, MA).

Synthesis of photolinker (Scheme 1)

IPS (1.34 mmol) and DBT (0.033 mmol) were dissolved in anhydrous ethyl acetate, then 4-[4-(1-hydroxyethyl)-2-methoxy-5-nitrophenoxy] butyric acid was added at 75 °C. After 48 h at 80 °C reflux, the solvent was evaporated and compound was purified by column chromatography using silica gel and 10 % potassium carbonate. Mixture of ethyl acetate:hexane = 3: 1(v/v) was used as an eluent, and yellow product was obtained. [17]

^{1}H NMR (500M Hz, $CDCl_3$): δ = 7.56 (s, Aromatic-**H**), δ = 6.98 (s, Aromatic-**H**), δ = 6.34 (q, Aromatic-C**H**(CH_3)-), δ = 4.10 (t, Aromatic-OC**H**$_2$), δ = 3.93 (s, Aromatic-OC**H**$_3$), δ = 3.81 (q, Si(OC**H**$_2$$CH_3$)), δ = 3.26 (m, Aromatic-CHO(C=O)NHC**H**$_2$), δ = 3.16 (m, Aromatic-$OCH_2CH_2CH_2CONHC$**H**$_2$), δ = 2.35 (m, Aromatic-OCH_2C**H**$_2CH_2CONH$), δ = 2.17 (t, Aromatic-OCH_2CH_2C**H**$_2CONH$), δ = 1.62 (dt, -C**H**$_2CH_2Si(OCH_2CH_3)_3$), δ =1.57 (d, Aromatic-CHC**H**$_3$,), δ = 1.25 (t, Si$(OCH_2C$**H**$_3)_3$), δ = 0.62 (t, -C**H**$_2Si(OCH_2CH_3)_3$).

Preparation of seed and nanoparticles

The seed and nanoparticles were prepared based on the method reported previously. [18, 19] Typically, 9.1 mg arginine was solved in 6.9 mL water and then 0.45 mL cyclohexane and 0.55 mL TEOS were added to the solution in this order. The solution was stirred at 60 °C for 20 h and the uniform size of the seed was prepared.

The solution of 100 μL seed, 100 μL arginine (10 mg/mL) in water, and encapsulated molecule (40 μL rhodamine B (10 mg/mL) or 100 μL Nile blue A (1 mg/mL) or 300 μL PI (50 μg/mL)) were added to 3 mL water. Then, 15 mg photolinker in ethanol (100μL) and 35.2 μL TEOS were added. The mixture solution was stirred with a speed of 300 rpm at 60 °C for 24 h and the diameter of the nanoparticles grew up till about 50 nm. The prepared nanoparticles were filtered through a vivaspin centrifugal filter (molecular weight cut off of 30k, Sartorius, Göttingen, Germany) to remove excess molecules which were not encapsulated in nanoparticles.

Surface modification of photodegradable silica nanoparticles

0.25 mL of the nanoparticles solution and 0.25 mL of R8 peptide (4 μM in water) were mixed and vortex for 20 min at room temperature.

Transmission electron microscopy (TEM) observation

TEM images were obtained with an H-7000 electron microscope (Hitachi, Tokyo, Japan) operating at 75 kV. Copper grids (400 mesh) were coated first with a thin film of collodion and then with carbon. The nanoparticle dispersion (5 μL) was placed on the coated copper grids.

Diameter and Zeta potential measurements by dynamic light scattering (DLS)

Delsa Nano (Beckman Coulter. Inc. Brea CA, USA) was used for the measurement of diameters and Zeta potentials of the prepared nanoparticles. The nanoparticle solution was diluted by water for diameter measurement or 10 mM NaCl solution for Zeta potential measurements.

Irradiation condition

UV curing equipment, Aicure UV20 (Panasonic, Osaka, Japan), was used as a light source for UV irradiation. The wavelength of the irradiating light was 365 nm at an intensity of 20 mW/cm^2. The irradiation times of the nanoparticles in a 0.6 mL microtube and those in cells were 1 min and 20 sec, respectively.

Measurement of released molecule

After the irradiation, nanoparticles solution was centrifuged at 120,000 rpm for 30 min using ultracentrifuge equipment (Optim TLX, Beckman Coulter, Inc. Brea, CA). The supernatants of the solution (100 μL) were moved to well of a microplate. 100 μL of 10 mM phosphate buffer (pH 7.4) for rhodamine B and Nile blue A assays or 100 μL of 0.2 mg/mL DNA solution for PI assay was added to each well before fluorescence measurement. The fluorescence (ex 570 nm, em 590 nm for rhodamine B: ex 635 nm, em 674 nm for Nile blue A: ex 530 nm, em 620 nm for PI: ex 480 nm, em 520 nm for BZAR) were measured with a multiplate reader (SH-9000, Corona Electric Co., Ibaraki, Japan).

Cell culture and the nanoparticles internalization to cells

The adenocarcinomic human alveolar basal epithelial (A549) cells were cultured in a humidified atmosphere of 95% air and

5% CO_2 at 37 °C in Dulbecco`s Modified Eagle`s Medium (DMEM, Sigma-Aldlich) supplemented with 1% (v/v) penicillin-streptomycin solution (x 100) (Wako) and 10% (v/v) fetal bovine serum (FBS, invitorogen). For each experiment, cells at 80-90 % confluence were harvested by trypsin/EDTA (Wako) digestion, washed and re-suspended in fresh growth medium with FBS at a cell concentration of 106 viable cells/culture dish (75 cm^2). All cells were cultured in 35 mm glass bottom dish.

For the internalization of the nanoparticles to cells, the cultured dish was washed by DMEM without FBS. Then, 200 μL of the nanoparticles solution was dropped to the dish and stand the dish for 1 hour at 37 °C for internalization. After that, the sample was washed 2 times by PBS. Then SYTO16 dye was added to the medium at a final concentration of 500 nM to stain the nucleus and incubated for 20 min at 37 °C. Cells were washed 3 times with PBS and supplied fresh DMEM before irradiation.

Microscopy observation

The confocal fluorescence microscopy images of the cells were obtained with an FV10i microscope (Olympus, Tokyo, Japan). The laser power of the microscopy was set at 40 %.

Fluorescence intensity analysis in nucleus

Fluorescence intensity within nucleus was evaluated by means of confocal laser scanning microscopy. The fluorescence intensity in the images was analyzed with ImageJ software (ver. 1.45s; http://rsbweb.nih.gov/ij/index.html). The mean gray value of each nucleus was calculated from three different areas in a nucleus. The average values were obtained from the mean gray values of 5 different cells.

Results and discussion

Preparation of photodegradable nanoparticles containing rhodamine B

First, we prepared silica-based photodegradable nanoparticles containing rhodamine B. The seed particles (27 nm in diameter) were prepared by the hydrolysis and condensation reactions of TEOS. Then the seed grew by the addition of rhodamine B, photolinker, and TEOS to the seed solution. To examine the influence of the nanoparticle composition on the release of the encapsulated molecule, we prepared two different nanoparticles: one containing the photolinker, and the other without the photolinker. The size and shape of nanoparticles were analyzed by means of DLS and TEM (Fig. 1). The shape, size distribution, and average size of the nanoparticles with or without the photolinker were similar. Both types of nanoparticle were spherical in shape and their size distributions were narrow (both types of particle were about 50 nm). These results indicate that the addition of the photolinker did not affect the formation of the nanoparticles.

Then, we compared the amount of rhodamine B released from these rhodamine B-encapsulated nanoparticles before and after UV irradiation (Fig. 2). The supernatant of rhodamine B for both types of nanoparticles showed very low fluorescence intensity before UV irradiation. However, after irradiation, the fluorescence intensity was increased (about 7 times) only for the rhodamine B encapsulated in the nanoparticles with the photolinker. Then, the excitation and emission spectra of rhodamine B, rhodamine B-encapsulated nanoparticle, and released rhodamine B were compared. Although the small shifts of the maximal excitation and emission wavelengths were observed for the nanoparticle, almost no shift of them was observed between the original rhodamine B and released

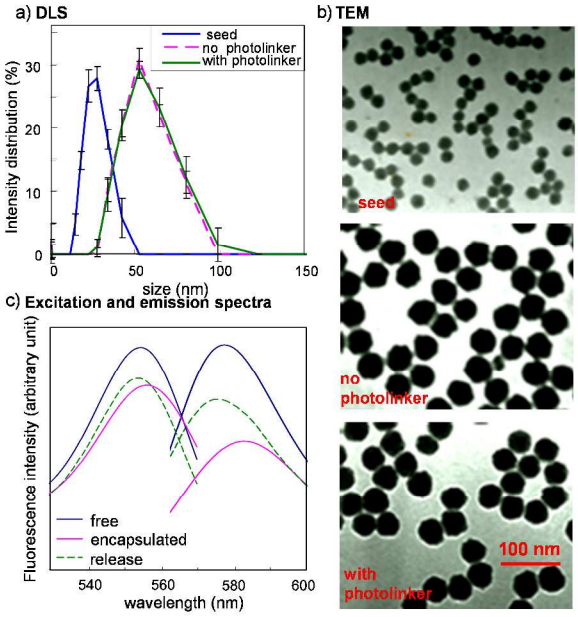

Fig. 1 a) DLS and b) TEM analysis of seed and nanoparticles with and without photolinker, and c) excitation and emission spectra of free rhodamine B, rhodamine B-encapsulated nanoparticle, and released rhodamine B.

rhodamine B (Fig. 1). These results demonstrate that rhodamine B encapsulated in the photodegradable nanoparticles could be released upon UV irradiation. Because the encapsulated molecule was immobilized by the mesh structure that was prepared by the polymerization reaction of the silica, this technique could be applicable to various kinds of molecules for their encapsulation and subsequent release by irradiation. Because the amount of released rhodamine B was estimated to be about 15 %, most of the rhodamine B remained in the nanopartiocles after irradiation.

Generality of the release technique

To examine the generality of this method, we also examined the controlled release of Nile blue A and PI, the release of which are difficult to control using PEG-based photodegradable gel. [8] The color of these compounds disappeared when they were encapsulated in PEG-based photodegradable nanoparticles, because of the reaction with ammonium peroxodisulfate. The released amount of Nile blue A was measured from the fluorescence intensity of the supernatant. The released amount of PI from the nanoparticles was measured by the fluorescence intensity of the complex of DNA and PI in the supernatant, because the fluorescence intensity of PI is changed by its intercalation with DNA. The release of these compounds from the nanoparticles into the supernatant was observed after irradiation (Fig. 2). The irradiation increased the fluorescence signals of the supernatants by 7- and 3-fold for Nile blue A and PI, respectively. The amounts of released Nile blue B and PI were estimated to be about 13 and 5 %, respectively, these molecules remained in the nanopartiocles after irradiation. It was supposed that this low released efficiency of PI was originated from many positive charges of PI than those of rhodamine B and Nile blue A.

The effect of the UV intensity on the release amount was examined. Four different UV intensities (30, 60, 120, and 250 mJ) were used to study. Figure 2 b) shows the relationship between the light intensity and the released amount observed after the irradiation. Predictably, the largest quantity was

obtained when the strongest intensity of UV light was used (250 mJ), and the quantity decreased with decreasing light intensity. A change of the nanoparticles that was derived from UV irradiation was observed by TEM observation (Fig. 2 c). Although the nanoparticle before the irradiation was spherical shape and the surface looked like smooth, the surface of the nanoparticle after the irradiation became rough. It was supposed that this rough surface was derived from many cracks formed by cleavage reaction of the nitrobenzyl group. These data suggest that silica nanoparticles could be used for the controlled release of various molecules, because small molecules whose release was difficult to control using PEG-based nanoparticles could be released from silica nanoparticles by use of irradiation.[6] This was derived from the mild preparation condition of the silica nanoparticles and small mesh of the nanoparticles.

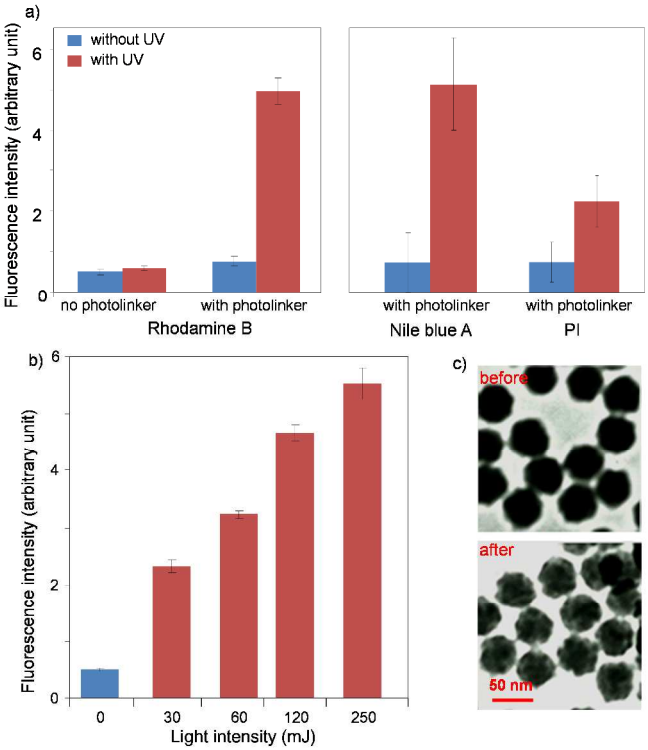

Fig. 2 a) Release of the encapsulated molecule from the nanoparticles with or without irradiation, b) relationship between irradiation power and released BZAR form the nanoparticles, and c) TEM images of nanoparticles before and after irradiation.

Surface modification of the nanoparticles

Nanoparticles containing a functional molecule can be used as a vehicle to transport that molecule, because nanoparticles can be delivered to various locations. After the nanoparticles reach a target site, the encapsulated molecule can be released and activated by light stimuli. Silica-based nanoparticles have been used to carry functional molecules into cells and the molecules within the cell then activated by irradiation because silica was thought to be a low immune response material. However, silica nanoparticles are not internalized into cells without first being modified with a membrane permeable peptide, such as R8 or HIV-1 Tat, to increase their uptake efficiency.[20-22] We analyzed the shape, size and Zeta potential of the modified nanoparticles

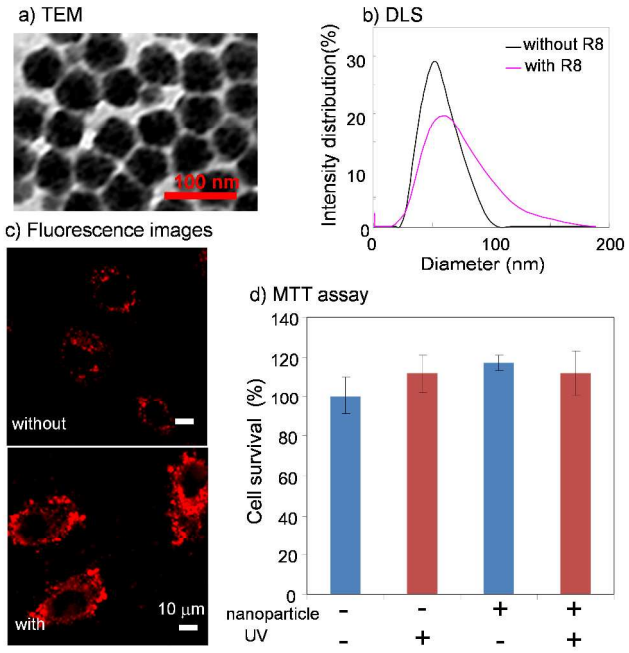

Fig. 3 a) TEM and b) DLS analysis of nanoparticles modified with R8 peptide, c) fluorescence images of A549 cells treated with PI-encapsulated nanoparticles modified with R8 peptide or without modification, and d) effect of nanoparticles and UV irradiation on cell survival.

by using TEM and DLS (Fig. 3 a and b). The shape of the nanoparticles was not changed by modifications (Fig. 1 and 3a), but the diameter range increased and the average diameter of the nanoparticles became about 60 nm. The values of the polydispersity index (PDI) of these nanoparticles were increased from 0.083 to 0.231. The modification with R8 peptide produced a large difference in the Zeta potential; the value was -29±6 mV before this modification and +15±1 mV after the modification. This charge difference of the nanoparticles increased their affinity for the cell surface, which is negatively charged. These results indicate that the surface of the nanoparticles was modified by the R8 peptide.

We then compared the internalization efficiencies of the nanoparticles with and without R8 modification. Both types of nanoparticles containing PI were prepared and added to the culture medium. The internalization efficiency of the unmodified nanoparticles was low, because less fluorescence signal was detected from the cells that were treated with the unmodified nanoparticles (Fig. 3c). On the other hand, most of the cells that were treated with the R8-modified nanoparticles showed fluorescence. This high internalization efficiency of R8-modified nanoparticles is consistent with previous reports.[20-22] Effect of UV irradiation and nanoparticles on the cell activity was examined using MTT assay. No deleterious effects by the irradiation and nanoparticles were observed (Fig. 3 d)).

Release of the encapsulated molecule within cells by irradiation

Then we tried to release the encapsulated molecule from the nanoparticles by using light stimuli within the cells. To observe the effect of the released molecule within the cell, we used nanoparticles containing PI. Red fluorescence was observed in

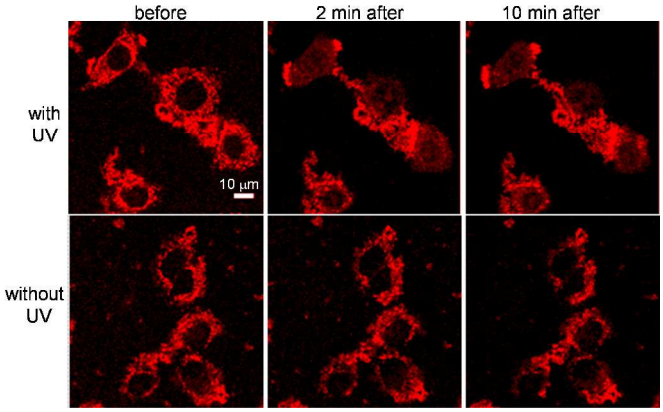

Fig. 4 Fluorescence images of A549 cells treated with nanoparticles containing PI. Upper and lower lanes show irradiated and nonirradiated cells.

the cytoplasm of the cells before the irradiation when the cells were treated with PI-encapsulated nanoparticles (Fig. 4). The strong signal could not be detected in the nucleus where PI generally localizes. This finding indicates that only the PI that was encapsulated in the nanoparticles was internalized into the cells. After irradiation, the red fluorescence signal was detected not only in the cytoplasm but also in the nucleus of the cells (Fig. 4 upper lane). This signal was derived from PI that was released from the nanoparticles and moved into the nucleus. The fluorescence signal that was still detectable in the cytoplasm was likely derived from PI that coexisted with degraded nanoparticles, because PI is a cationic compound that interacts with silica gel via electrostatic interactions even after the collapse of the nanoparticles. No change was observed with the nonirradiated cells; the red fluorescence remained in the cytoplasm of the cells (Fig. 4 lower lane). In general, PI localizes to the nucleus and intercalates with DNA when it is internalized into a cell,[23] but the PI within the nanoparticles could not reach the nucleus when it was wrapped in 60-nm-sized nanoparticles, because the PI-encapsulated nanoparticles could not penetrate the 10-nm-sized nuclear pore.[24] When the PI was released from the nanoparticles by irradiation, the PI molecules could pass through the nuclear pore and intercalate with DNA, causing the red fluorescence seen in the nucleus. In addition, the light irradiation did not cause serious damage to the cells, because our cell survival assessment showed no substantial changes. Therefore, these data demonstrate that photodegradable silica nanoparticles can be used to control the release of encapsulated molecules within a cell.

Finally, we examined the time course of the fluorescence changes in the nucleus. We found that the red fluorescence signal in the nucleus started to increase within 2 min after the irradiation treatment and became stable at around 8 min (Fig. 5). No further changes in fluorescence intensity were observed in the nucleus for more than one hour. Because our previous study showed that molecules released from nanoparticles within the cell distribute throughout the cell and reach an equilibrium state within 10 min,[9] the 8-min timeframe for the distribution of the released PI by diffusion and subsequent localization to the nucleus seemed reasonable. The release of the PI was quick and transient, because the fluorescence intensity in the nucleus stabilized quickly. To examine the effect of releasing molecule within a cell, a rapid and transient release is necessary because the effect disappears within the approximately 10 min timeframe it takes to reach an equilibrium state. We believe that these nanoparticles represent a very promising tool to clarify the effect of released molecules within cells and to control cellular functions using released molecules.

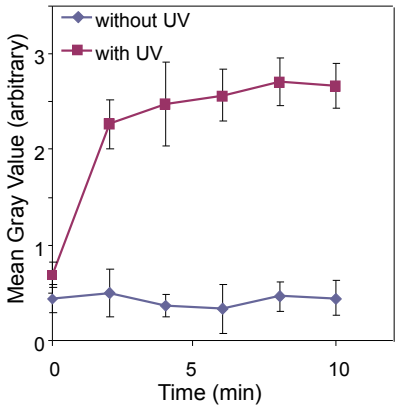

Fig. 5 Time-dependent fluorescence changes in the nucleus of A549 cells after with or without irradiation.

Conclusions

We developed a method to control molecular function by using photodegradable silica-based nanoparticles. The nanoparticles were effective tools to functionally control small molecules, because the mesh size of the nanoparticle gel was small and no radical polymerization was needed to prepare the nanoparticles. Surface modification of the nanoparticles with R8 permitted the nanoparticles to be internalized strongly into the cells and deliver the encapsulated molecule to the cytoplasm. The nanoparticles released the encapsulated molecule quickly and transiently on exposure to a short burst of irradiation. Given that many researchers are interested in the local cellular functions of molecules, these nanoparticles should be broadly applicable to such research. Drug delivery systems and photoactivated sensors are other promising areas for the application of nanoparticles, because the timing of release can be controlled precisely with light stimuli.

Acknowledgements

We thank Dr. S. Fukuda (U. Tokyo), Mr. T. Tsuboya (U. Tokyo) and Dr. N. Kaji (Nagoya Univ.) for technical assistances for TEM measurement, for cell study and for donating R8 peptide, respectively. This work was supported by grants (Kakenhi) from the Ministry of Education, Culture, Sports, Science, and Technology (MEXT) of Japan, JSPS Core-to-Core Program, A. Advanced Research Networks, and the Naito Foundation.

Notes and references

[a] Graduate School of Pharmaceutical Sciences and GPLLI Program, The University of Tokyo, 7-3-1 Hongo, Bunkyo-ku, Tokyo 113-0033, Japan
[b] Center for Medical Systems Innovation Summer Internship Program, The University of Tokyo, Japan
[#] Present address: Molecular Imaging Center, National Institute of Radiological Sciences, 4-9-1, Anagawa, Inage-ku, Chiba 263-8555, Japan

† Electronic Supplementary Information (ESI) available: [details of any supplementary information available should be included here]. See DOI: 10.1039/b000000x/

1 ES. Gil, SM. Hudson, *Prog. Poly. Sci*. 2004, **29**, 1173-1222.
2 S. Ganta, H. Devalapally, A. Shahiwala, M. Amiji, *J. Cont. Rel.* 2008, **126**, 187-204.
3 D.A.Giljohann, D.S. Seferos, A.E. Prigodich, P.C. Patel, C.A. Mirkin, *J. Am. Chem. Soc*. 2009, **131**, 2072-2073.
4 M.Naito, T. Ishii, A. Matsumoto, K. Miyata, Y. Miyahara, K. Kataoka, *Angew. Chem. Int. Ed.* 2012, **51**, 10751-10755.
5 M. J. Evans, M. H. Kaufman, *Nature*, 1981, **292**, 154–156.
6 S. Murayama, M. Kato, *Anal. Chem*. 2010, **82**, 2186-2191.
7 S. Murayama, B. Su, K. Okabe, A. Kishimura, K. Osada, M. Miura, T. Funatsu, K. Kataoka, M. Kato, *Chem. Commun.* 2012, **48**, 8380-8382.
8 S. Murayama, F. Ishizuka, K. Takagi, H. Inoda, A. Sano, T. Santa, M. Kato, *Anal. Chem*. 2012, **84**, 1374-1379.
9 K. Takagi, S. Murayama, T. Sakai, M. Asai, T. Santa, M. Kato, *Soft Mater*, DOI:10.1039/C3SM52908H.
10 S. Murayama, T. Nishiyama, K. Takagi, F. Ishizuka, T. Santa, M. Kato, *Chem. Commun*. 2012, **48**, 11461-11463.
11 S. Murayama, J. Jo, Y. Shibata, K. Liang, T. Santa, T. Saga, I. Aoki, M. Kato, *J. Mater. Chem. B* 2013, **1**, 4932-4938.
12 S. Murayama, P. Kos, K. Miyata, K. Kataoka, E. Wagner, M. Kato, *Macromolecular Bioscience*, DOI: 10.1002/mabi.201300393.
13 M. Kato, K. Sakai-Kato, N. Matsumoto, T. Toyo'oka, *Anal. Chem.* 2002, **74**, 1915-1921.
14 M. Kato, K. Sakai-Kato, H.-M. Jin, K. Kubota, H. Miyano, T. Toyo'oka, M. T. Dulay, R. N. Zare, *Anal. Chem*. 2004, **76**, 1896-1902.
15 K. Sakai-Kato, M. Kato, H. Homma, T. Toyo'oka, N. Utsunomiya-Tate, *Anal. Chem.* 2005, **77**, 7080-7083.
16 K. Sakai-Kato, M. Kato, T. Toyo'oka, *J. Chromatogr. A* 2004, **1051**, 261-266.
17 D.C. Harrowven, D.P. Curran, S.L. Kostiuk, I.L. Wallis-Guy, S. Whiting, K.J. Stenning, B. Tang, E. Packarda, L. Nansona, *Chem. Commun*. 2010, **46**, 6335-6337.
18 T. Yokoi, Y. Sakamoto, O. Terasaki, Y. Kubota, T. Okubo, T. Tatsumi, *J. Am. Chem. Soc.* 2005, **128**, 13664-13665.
19 T. Yokoi, J. Wakabayashi, Y. Otsuka, W. Fan, M. Iwama, R. Watanabe, K. Aramaki, A. Shimojima, T. Tatsumi, T. Okubo, *Chem. Mater.* 2009, **21**, 3719-3729.
20 I. Nakase, H. Akita, K. Kogure, A. Graslund, U. Langel, H. Harashima, S. Futaki, *Acc. Chem. Res*. 2012, **45**, 1132-1139.
21 H. Yukawa, Y. Kagami, M. Watanabe, K. Oishi, Y. Miyamoto, Y. Okamoto, M. Tokeshi, N. Kaji, H. Noguchi, K. Ono, M. Sawada, Y. Baba, N. Hamajima, S. Hayashi, *Biomat.* 2010, **31**, 4094-4103.
22 H. Akita, R. Ito, IA. Khalil, S. Futaki, H. Harashima, *Mol. Ther.* 2004, **9**, 443-451.
23 I. W. Taylor, B. K. Milthorpe, *J. Histochem. Cytochem*. 1980, **28**, 1224-1232.
24 N. Panté, M. Kann, *Mol. Biol. Cell* 2002, **13**, 425–434.

